Optik - International Journal for Light and Electron Optics 224 (2020) 165503

Contents lists available at ScienceDirect

Optik

journal homepage: www.elsevier.com/locate/ijleo

Original research article

Strain engineering of the electro-optical and photocatalytic properties of single-layered Janus MoSSe: First principles calculations

Thi-Nga Do [a,b], Chuong V. Nguyen [c], M. Idrees [d], Bin Amin [e], Ho A. Tam [f], Nguyen N. Hieu [g,h], Huynh V. Phuc [i], Le T. Hoa [g,h,*]

[a] Laboratory of Magnetism and Magnetic Materials, Advanced Institute of Materials Science, Ton Duc Thang University, Ho Chi Minh City, Viet Nam
[b] Faculty of Applied Sciences, Ton Duc Thang University, Ho Chi Minh City, Viet Nam
[c] Department of Materials Science and Engineering, Le Quy Don Technical University, Ha Noi, Viet Nam
[d] Department of Physics, Hazara University, Mansehra 21300, Pakistan
[e] Department of Physics, Abbottabad University of Science and Technology, Abbottabad 22010, Pakistan
[f] Laboratory for Micro-Nano Technology, VNU University of Engineering and Technology Vietnam National University, Hanoi 10000, Viet Nam
[g] Institute of Research and Development, Duy Tan University, Da Nang 550000, Viet Nam
[h] Faculty of Natural Sciences, Duy Tan University, Da Nang 550000, Viet Nam
[i] Division of Theoretical Physics, Dong Thap University, Dong Thap, Viet Nam

ARTICLE INFO

Keywords:
Janus MoSSe
2D materials
DFT calculations
Band alignment

ABSTRACT

In present work, we study the electronic, optical and photocatalytic properties of strained MoSSe monolayer through first-principles study. A single layer Janus MoSSe possesses a semiconducting character with a direct band gap of 1.59/2.09 eV obtained by PBE/HSE06 method. The valence band maximum (VBM) of Janus MoSSe monolayer is mainly contributed by the S-*p* orbital, whereas the conduction band minimum (CBM) comes from the Mo-d_{x^2}. Furthermore, Janus MoSSe monolayer has been proved to be energetically stable with no imaginary frequency in its phonon spectrum. Interesting, both the tensile and compressive strains can transform Janus MoSSe monolayer from direct to indirect band gap nature as well as tune its band gap. The compressive strain tends to an increase in the band gap, whereas the tensile strain leads to decrease in the band gap. Optical absorption of Janus MoSSe monolayer demonstrates that the tensile strain gives rise to an existence of blue shift, while compressive strain is responsible for the formation of a red shift. Photocatalytic properties show that Janus MoSSe monolayer with 4% or 6% strained could be a catalyst for the H_2O oxidation, making it suitable for water splitting applications.

1. Introduction

Besides graphene, two-dimensional (2D) transition metal dichalcogenides (TMDCs) have recently considered much interest due to their technological applications [1–6]. The promising properties of 2D TMDCs from their bulk creates additional important. For example, the indirect band gap nature in bulk MoS_2 and WS_2 can be converted into direct band gap semiconductors in their monolayer

* Corresponding author at: Institute of Research and Development, Duy Tan University, Da Nang 550000, Viet Nam.
E-mail addresses: dothinga@tdtu.edu.vn (T.-N. Do), lethihoa8@duytan.edu.vn (L.T. Hoa).

https://doi.org/10.1016/j.ijleo.2020.165503
Received 19 May 2020; Received in revised form 17 August 2020; Accepted 22 August 2020
Available online 28 August 2020

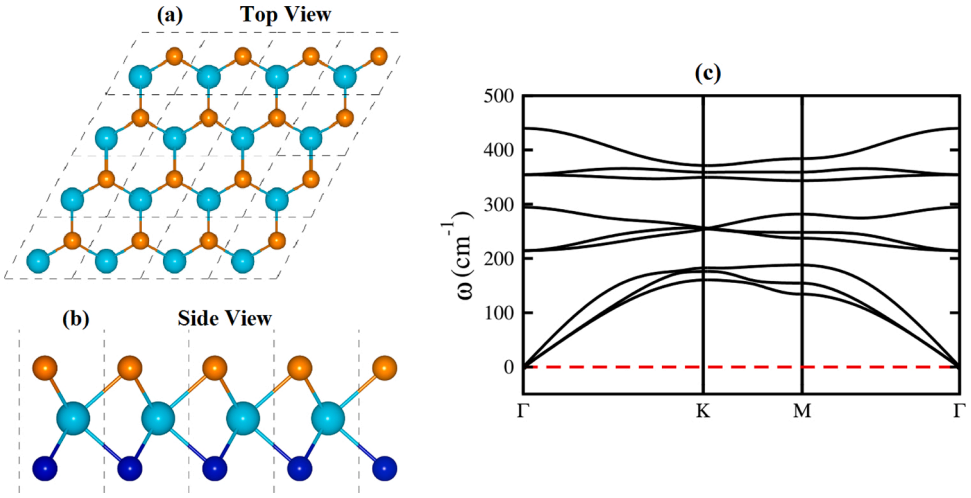

Fig. 1. (a) Top view (b) side view and (c) phonon dispersion curves of Janus MoSSe monolayer after relaxation.

forms. Moreover, many strategies, including doping [7], making alloys [8–13], strain engineering [14], and constructing heterostructures [15,16] have been also devoted to enhance the properties and applications of 2D materials. Among these, strain engineering is proved to be one of the most efficient strategies for improving the performance of electronic devices. Experimentally, strain effect could be generated by external loading or epitaxy on 2D compounds in order to tune the structural, electronic, and catalytic properties of materials [17,18]. Recently, a new 2D group known as Janus TMDCs has been devolved from selenization and sulfurization in MoS_2 and $MoSe_2$ [19,20]. Electronic structures and Raman modes of Janus MoSSe monolayer obtained from density functional theory (DFT) show excellent agreement with experimental results [20]. Janus 2D materials are also useful for spintronic devices due to the large spin–orbit coupling (SOC) and Rashba spin splitting [21]. On the theoretical side, Xia et al. [22] predicted that Janus MXY (M = Mo, W; X, Y = S, Se, Te) have many advantages that merit for high-efficient photocatalysts.

Up to now, the effects of both uniaxial and biaxial strains on the structural, electronic and vibrational properties as well as band offsets of 2D TMDCs have been investigated [23–26]. It is obvious that the properties of 2D TMDCs are very sensitive to the strain engineering, implying that they are promising candidates for the fields of optoelectronics and nanoelectronics. As for Janus TMDCs, their electronic, optical, and mechanical properties have also been studied theoretically [27–30].

Recently, quasiparticle band structures and optical properties of MX_2 (M = Mo, W, X = S, Se, Te) monolayers have been explored by GW approximation in conjunction with the Bethe–Salpeter equation [31,26]. Especially, the roles played by strain engineering on these properties have also been addressed [25]. However to our knowledge, no investigation about the variation of band structure, effective mass, photocatalytic response and optical properties of Janus MoSSe monolayers under strain has been carried out up to this point of time [25]. Therefore, in this work using density functional theory (DFT), a comprehensive insight is gained into the effect of strain engineering on the electronic structure, effective masses, optical properties and photocatalytic performance of the Janus MoSSe. We also discuss the valence and conduction band edge potentials to find out their possible applications in photocatalytic.

2. Computational methods

In this work, the electronic properties of Janus MoSSe monolayer is computed by using the first-principles calculations based on density functional theory, which is implemented in plane-wave basic QUANTUM ESPRESSO package [32]. The Perdew-Burke–Ernserhof (PBE) functional in the generalized gradient approximation (GGA) [33] is used to describe the exchange correlation functional. The energy cutoff is set to 500 eV for plane wave expansion and the first Brillouin zone is represented by $12 \times 12 \times 1$ Monkhorst Pack k-point grid. The optimized atomic positions are procured when the threshold for energy and forces is less than 10^{-6} eV and 10^{-4} eV/Å, respectively. In addition, 86 uniform k-points along the high-symmetry special k-paths are used to obtain the band structure. The hybrid functional Heyd–Scuseria–Ernzerhof (HSE06) [34] was also adopted to acquire more accurate band gap. The DFT-D2 method [35] is also taken into account for exacting the weak van der Waals interaction. All the entities are provided with a vacuum level of 24 Å along the z direction in order to avoid factitious interactions between the layers of atoms. Phonon dispersion spectrum is calculated by using harmonic interatomic force constants as determined by the density functional perturbation theory while holding with a $4 \times 4 \times 1$ supercell.

3. Results and discussion

We first examine the atomic structure of Janus MoSSe monolayer, in which the Mo atom is sandwiched between S and Se atoms, as depicted in Fig. 1. The lattice constant after full relaxation is computed to be 3.25 Å. Our calculations of bond lengths give the values of 2.43 Å for Mo–S and 2.52 Å for Mo–Se, while it is 3.32 Å for the nearest distance of S–Se. These results are in good agreement with

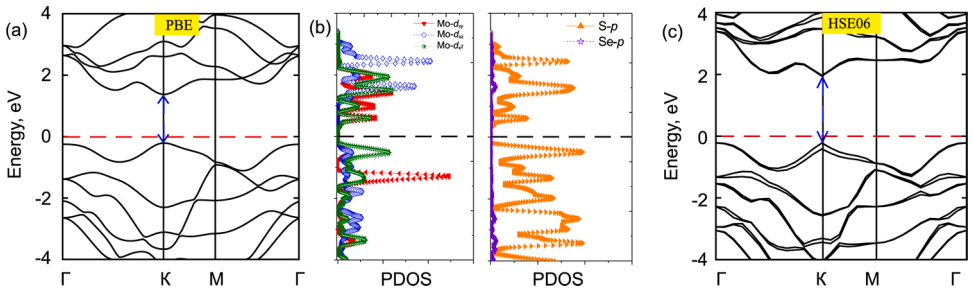

Fig. 2. Band structures of Janus MoSSe monolayer obtained by (a) PBE and (c) HSE06 calculations. (b) Partial density of states (PDOS) of Janus MoSSe monolayer at the equilibrium state.

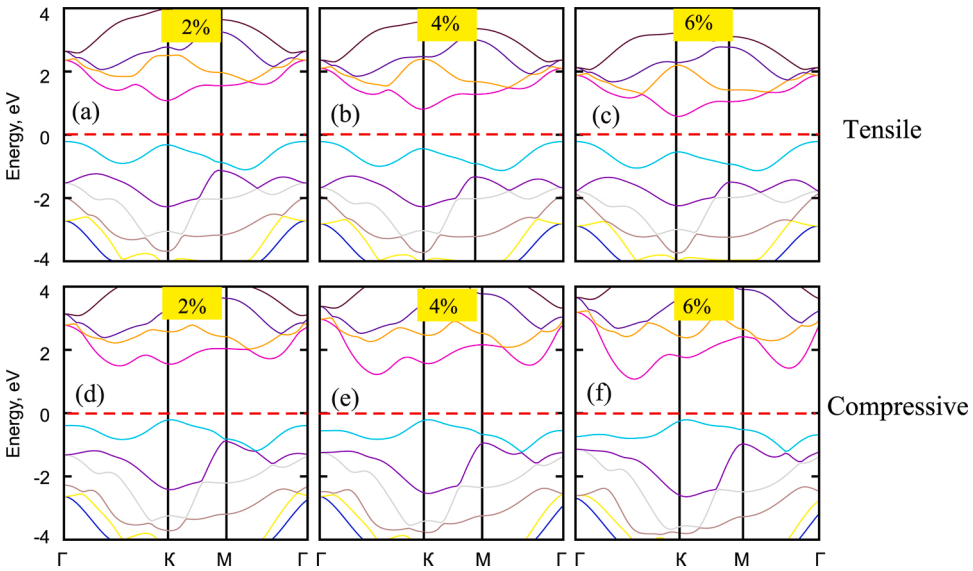

Fig. 3. Band structures of Janus MoSSe monolayer under different tensile strains of (a) 2%, (c) 4%, (c) 6% and compressive strains of (d) 2%, (e) 4% and (f) 6%, respectively.

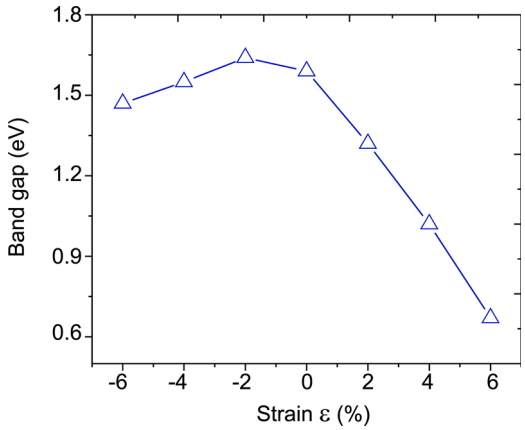

Fig. 4. Band gap variation of Janus MoSSe monolayer as a function of strains.

previous reports [36,37], confirming the reliability of our approach. Furthermore, in order to verify the structural stability of Janus MoSSe monolayer, we calculate its phonon dispersion curves, as shown in Fig. 1(c). We find that the phonon spectrum of Janus MoSSe monolayer contains no imaginary soft modes with negative frequency, indicating its structural stability.

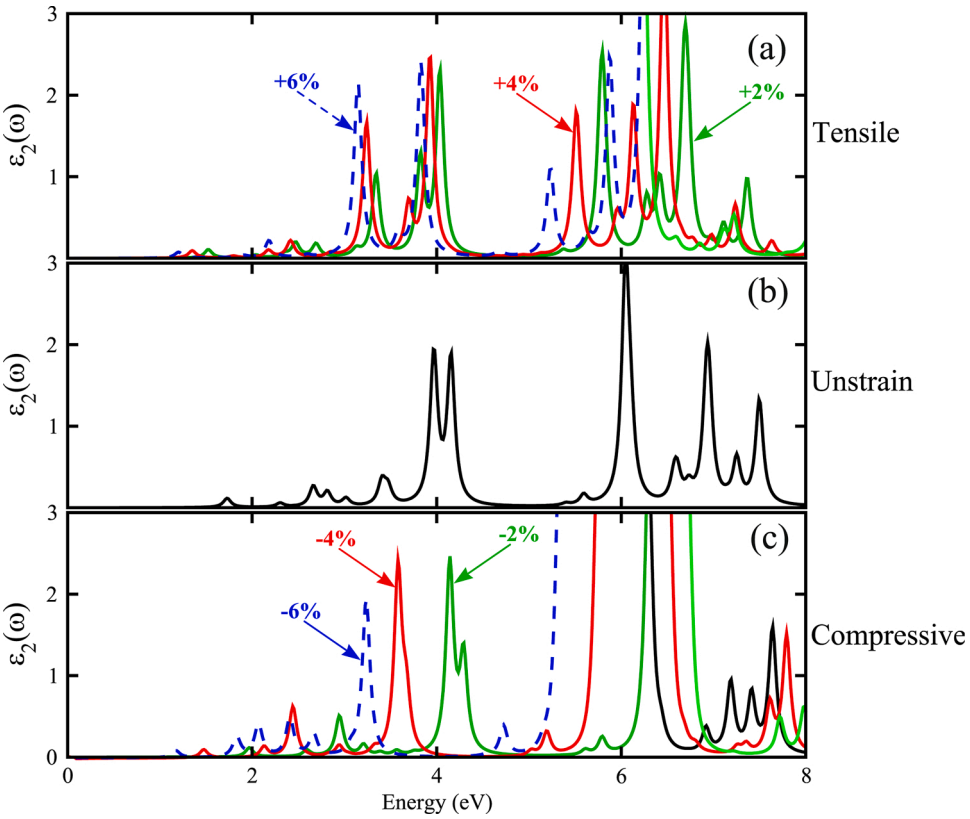

Fig. 5. Imaginary part of dielectric function of Janus MoSSe under (a) tensile strain, (b) unstrained (c) compressive strain.

The electronic band structures and partial density of states (PDOS) of Janus MoSSe monolayer are calculated and plotted in Fig. 2. At the ground state, this material possesses a direct band nature of semiconductor. Both the VBM and CBM are located right at K point. The band gap of Janus MoSSe monolayer calculated by PBE and HSE06 are 1.59 and 2.09 eV, respectively. These results are consistent with the previous theoretical report [37,38]. One can find that as compared to the experimental band gap of MoSSe monolayer of 1.68 eV [19], the PBE calculation underestimates the band gap by 0.09 eV, whereas the HSE06 over estimates the band gap by 0.41 eV. Both the PBE and HSE06 calculations predict the same trend in the electronic band structures of Janus MoSSe monolayer. Therefore, we further calculate the electronic properties of Janus MoSSe monolayer using PBE calculation. The partial density of states (PDOS) of all atoms in Janus MoSSe monolayer are displayed in Fig. 2(b). Our calculations show that the VBM is mainly contributed by the S-*p* orbital, whereas the CBM comes from the Mo-d_{x^2}.

As is well known that the strain is the most common approach to tune the band gap value of materials. Thus, to modulate the band gap of simple TMDC monolayers a very small strain is required, which is in sharp contrast with that of grapheme [23]. Here, we apply both the compressive and tensile strains to Janus MoSSe monolayer in order of 2% by setting the calculated lattice parameter to a fixed smaller or larger values and relaxing the atomic positions. The effect of a compressive strain decreases the bond length and thus enhances coupling, giving rise to the increase in bonding–antibonding splitting. The opposite is true for the tensile strain.

The band gap and band structures of Janus MoSSe monolayer under tensile and compressive strains are illustrated in Figs. 3 and 4 . One can find from Fig. 3(a)-(c) that the tensile strain leads to the decrease in the band gap of Janus MoSSe monolayer. With increasing the tensile strain from 2% to 4% and to 6%, the band gap of MoSSe monolayer decreases from 1.32 to 1.02 eV and to 0.76 eV, respectively. More interestingly, we find that under the tensile strain of 2%, the VBM shifts from *K* point to Γ point, whereas the CBM maintains at *K* point, resulting in the transition from direct to indirect band gap. By increasing the tensile strain up to 6%, the Janus MoSSe monolayer becomes an indirect band gap semiconductor. In fact, the decrease in the band gap of Janus MoSSe monolayer under tensile strain is due to the shift of the Fermi level towards the CBM.

The calculated band structures of Janus MoSSe monolayer under compressive strain are depicted in Fig. 3(d)–(f). We find that the band gap of Janus MoSSe monolayer firstly increases to 1.64 eV with increasing the compressive strain to −2%. Then the band gap decreases to 1.55 and 1.47 eV with further increasing the compressive strain to −4% and −6%, respectively. A similar trend of strain effect on the band gap was also observed in other Janus monolayers [39]. Under the compressive strain, the VBM remains at *K* point, however, the CBM shifts from *K* point to the Γ–*K* path, resulting in the direct–indirect band gap transition. Therefore, we can conclude that the strain engineering can be used to tune the band gap and transition from direct to indirect in Janus MoSSe monolayer. This finding demonstrates that the Janus MoSSe monolayer could be used as a promising candidate for wide range applications.

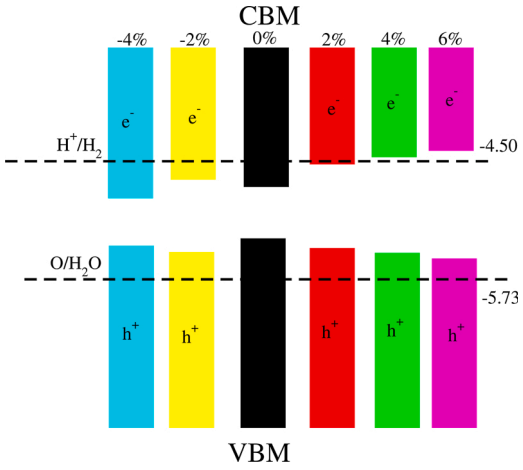

Fig. 6. Valence and conduction band edges of Janus MoSSe monolayer under different strain values.

The imaginary part of the dielectric function $\varepsilon_2(\omega)$ of unstrained and strained Janus MoSSe monolayer is shown in Fig. 5. Our results signify that the lowest energy transitions are dominated by excitons. The first higher peak for unstrained MoSSe is at 3.9 eV while for tensile (compressive) strain this peak locates at 3.39 (4.10), and 3.25 (4.3) eV and 3.16 (4.6) eV, respectively, for 2%, 4% and 6%. Moreover, by applying the tensile strain, the blue shift is observed while the compressive strain gives rise to the red shift. The red or blue shift is a quantum phenomenon, which describes the situation when an incident light contacts with the material, it either gains or loses some quanta by interacting with the vibrational modes of the material. When higher energy absorption takes place due to exciton, it leads a shift towards smaller wavelength (high energy) blue shift, and when energy is lost, a red shift is observed. These values indicate strong modifications in the positions of excitons in strained systems with respect to the parent monolayer systems. The blue/red shift further strengthen when the tensile/compressive strain is applied, which is consistent with the previous report [14]. This suggests that moderate strain holds promise for controlling the exciton–phonon interaction or coupling on the nanoscale.

Valence and conduction band edge potentials are used to investigate the photocatalytic properties of Janus MoSSe under strain by means of the Mulliken electronegativity $E_{VBM} = \chi - E_{elec} + 0.5 \times E_g$ and $E_{CBM} = E_{VBM} - E_g$. In this equation, χ denotes the geometric mean of the Mulliken electronegativity of the corresponding atoms, and E_g is the calculated band gap of Janus MoSSe monolayer by PBE method. For VB and CB we fix the Fermi level to −4.44 eV. We find that all the system fails for reduction and oxidation potential levels, while tensile strain of 4% and 6% shows good agent for reduction (Fig. 6).

4. Conclusions

In conclusion, the structural, electronic, optical and photocatalytic properties of Janus MoSSe monolayer under tensile and compressive strains have been investigated using density functional theory. Phonon spectra exhibit no imaginary frequency, confirming that MoSSe monolayer is thermally and dynamically stable. The Janus MoSSe monolayer possesses a semiconducting nature with a direct band gap of 1.59/2.09 eV obtained by PBE/HSE06 method. The strain engineering can tune the band gap and transition from direct to indirect. The blue and red shifts are observed by applying the tensile and compressive strains, respectively. Photocatalytic properties show that Janus MoSSe monolayer with 4% or 6% strained could be a catalyst for the H_2O oxidation, making it promising candidate for water splitting applications.

Declaration of Competing Interest

The authors report no declarations of interest.

References

[1] K. Xu, Z. Wang, X. Du, M. Safdar, C. Jiang, J. He, Atomic-layer triangular WSe_2 sheets: synthesis and layer-dependent photoluminescence property, Nanotechnology 24 (46) (2013) 465705.
[2] S. Bhattacharyya, A.K. Singh, Semiconductor-metal transition in semiconducting bilayer sheets of transition-metal dichalcogenides, Phys. Rev. B 86 (7) (2012) 075454.
[3] Y. Zhao, Y. Zhang, Z. Yang, Y. Yan, K. Sun, Synthesis of MoS_2 and MoO_2 for their applications in h2 generation and lithium ion batteries: a review, Sci. Technol. Adv. Mater. 14 (4) (2013) 043501.
[4] Y. Li, H. Wang, L. Xie, Y. Liang, G. Hong, H. Dai, MoS_2 nanoparticles grown on graphene: an advanced catalyst for the hydrogen evolution reaction, J. Am. Chem. Soc. 133 (19) (2011) 7296–7299.
[5] B. Xue, V. Nazabal, M. Piasecki, L. Calvez, A. Wojciechowski, P. Rakus, P. Czaja, I. Kityk, Photo-induced effects in GeS_2 glass and glass-ceramics stimulated by green and IR lasers, Mater. Lett. 73 (2012) 14–16.
[6] Q.H. Wang, K. Kalantar-Zadeh, A. Kis, J.N. Coleman, M.S. Strano, Electronics and optoelectronics of two-dimensional transition metal dichalcogenides, Nat. Nanotechnol. 7 (11) (2012) 699.

[7] H.-P. Komsa, J. Kotakoski, S. Kurasch, O. Lehtinen, U. Kaiser, A.V. Krasheninnikov, Two-dimensional transition metal dichalcogenides under electron irradiation: defect production and doping, Phys. Rev. Lett. 109 (3) (2012) 035503.
[8] H.-P. Komsa, A.V. Krasheninnikov, Electronic structures and optical properties of realistic transition metal dichalcogenide heterostructures from first principles, Phys. Rev. B 88 (8) (2013) 085318.
[9] S. Hadji, A. Bouhemadou, K. Haddadi, D. Cherrad, R. Khenata, S. Bin-Omran, Y. Al-Douri, Elastic, electronic, optical and thermodynamic properties of Ba3Ca2Si2N6 semiconductor: First-principles predictions, Phys. B: Condens. Matter (2020) 412213.
[10] Y. Al-Douri, M. Ameri, A. Bouhemadou, K.M. Batoo, First-principles calculations to investigate the refractive index and optical dielectric constant of Na3SbX4 (X = S, Se) ternary chalcogenides, Phys. Stat. Sol. B 256 (11) (2019) 1900131.
[11] K. Boudiaf, A. Bouhemadou, Y. Al-Douri, R. Khenata, S. Bin-Omran, N. Guechi, Electronic and thermoelectric properties of the layered BaFAgCh (Ch = S, Se and Te): first-principles study, J. Alloys Compd. 759 (2018) 32–43.
[12] A. Bekhti-Siad, K. Bettine, D.P. Rai, Y. Al-Douri, X. Wang, R. Khenata, A. Bouhemadou, C.H. Voon, Electronic, optical and thermoelectric investigations of zintl phase AE3AlAs3 (AE = Sr, Ba): first-principles calculations, Chin. J. Phys. 56 (3) (2018) 870–879.
[13] S. Touam, R. Belghit, R. Mahdjoubi, Y. Megdoud, H. Meradji, M.S. Khan, R. Ahmed, R. Khenata, S. Ghemid, D.P. Rai, Y. Al-Douri, First-principles computations of $Y_xGa_{1x}As$-ternary alloys: a study on structural, electronic, optical and elastic properties, Bull. Mater. Sci. 43 (1) (2020) 22.
[14] B. Amin, T.P. Kaloni, U. Schwingenschlögl, Strain engineering of WS_2, WSe_2, and WTe_2, RSC Adv. 4 (65) (2014) 34561–34565.
[15] B. Amin, N. Singh, U. Schwingenschlögl, Heterostructures of transition metal dichalcogenides, Phys. Rev. B 92 (7) (2015) 075439.
[16] B. Amin, T.P. Kaloni, G. Schreckenbach, M.S. Freund, Materials properties of out-of-plane heterostructures of MoS_2-WSe_2 and WS_2-$MoSe_2$, Appl. Phys. Lett. 108 (6) (2016) 063105.
[17] J. Li, Z. Shan, E. Ma, Elastic strain engineering for unprecedented materials properties, MRS Bull. 39 (2) (2014) 108–114.
[18] H. Sahin, S. Tongay, S. Horzum, W. Fan, J. Zhou, J. Li, J. Wu, F. Peeters, Anomalous Raman spectra and thickness-dependent electronic properties of WSe_2, Phys. Rev. B 87 (16) (2013) 165409.
[19] A.-Y. Lu, H. Zhu, J. Xiao, C.-P. Chuu, Y. Han, M.-H. Chiu, C.-C. Cheng, C.-W. Yang, K.-H. Wei, Y. Yang, et al., Janus monolayers of transition metal dichalcogenides, Nat. Nanotechnol. 12 (8) (2017) 744–749.
[20] J. Zhang, S. Jia, I. Kholmanov, L. Dong, D. Er, W. Chen, H. Guo, Z. Jin, V.B. Shenoy, L. Shi, et al., Janus monolayer transition-metal dichalcogenides, ACS Nano 11 (8) (2017) 8192–8198.
[21] Q.-F. Yao, J. Cai, W.-Y. Tong, S.-J. Gong, J.-Q. Wang, X. Wan, C.-G. Duan, J. Chu, Manipulation of the large Rashba spin splitting in polar two-dimensional transition-metal dichalcogenides, Phys. Rev. B 95 (16) (2017) 165401.
[22] C. Xia, W. Xiong, J. Du, T. Wang, Y. Peng, J. Li, Universality of electronic characteristics and photocatalyst applications in the two-dimensional Janus transition metal dichalcogenides, Phys. Rev. B 98 (16) (2018) 165424.
[23] C.-H. Chang, X. Fan, S.-H. Lin, J.-L. Kuo, Orbital analysis of electronic structure and phonon dispersion in MoS_2, $MoSe_2$, WS_2, and WSe_2 monolayers under strain, Phys. Rev. B 88 (19) (2013) 195420.
[24] J. Kang, S. Tongay, J. Zhou, J. Li, J. Wu, Band offsets and heterostructures of two-dimensional semiconductors, Appl. Phys. Lett. 102 (1) (2013) 012111.
[25] E. Scalise, M. Houssa, G. Pourtois, V. Afanasev, A. Stesmans, Strain-induced semiconductor to metal transition in the two-dimensional honeycomb structure of MoS_2, Nano Res. 5 (1) (2012) 43–48.
[26] P. Johari, V.B. Shenoy, Tuning the electronic properties of semiconducting transition metal dichalcogenides by applying mechanical strains, ACS Nano 6 (6) (2012) 5449–5456.
[27] W. Shi, Z. Wang, Mechanical and electronic properties of Janus monolayer transition metal dichalcogenides, J. Phys. Condens. Matter 30 (21) (2018) 215301.
[28] H.R. Jappor, M.M. Obeid, T.V. Vu, D. Hoat, H.D. Bui, N.N. Hieu, S.J. Edrees, Y. Mogulkoc, R. Khenata, Engineering the optical and electronic properties of Janus monolayer ga2sse by biaxial strain, Superlatt. Microstruct. 130 (2019) 545–553.
[29] H.D. Bui, H.R. Jappor, N.N. Hieu, Tunable optical and electronic properties of Janus monolayers Ga_2SSe, Ga_2STe, and Ga_2SeTe as promising candidates for ultraviolet photodetectors applications, Superlatt. Microstruct. 125 (2019) 1–7.
[30] S.-D. Guo, Phonon transport in Janus monolayer MoSSe: a first-principles study, Phys. Chem. Chem. Phys. 20 (10) (2018) 7236–7242.
[31] A. Ramasubramaniam, Large excitonic effects in monolayers of molybdenum and tungsten dichalcogenides, Phys. Rev. B 86 (11) (2012) 115409.
[32] P. Giannozzi, S. Baroni, N. Bonini, M. Calandra, R. Car, C. Cavazzoni, D. Ceresoli, G.L. Chiarotti, M. Cococcioni, I. Dabo, et al., Quantum espresso: a modular and open-source software project for quantum simulations of materials, J. Condens. Matter Phys. 21 (39) (2009) 395502.
[33] J.P. Perdew, K. Burke, M. Ernzerhof, Generalized gradient approximation made simple, Phys. Rev. Lett. 77 (18) (1996) 3865.
[34] J. Heyd, G.E. Scuseria, M. Ernzerhof, Hybrid functionals based on a screened coulomb potential, J. Chem. Phys. 118 (18) (2003) 8207–8215.
[35] S. Grimme, Semiempirical GGA-type density functional constructed with a long-range dispersion correction, J. Comput. Chem. 27 (15) (2006) 1787–1799.
[36] M. Idrees, H. Din, R. Ali, G. Rehman, T. Hussain, C. Nguyen, I. Ahmad, B. Amin, Optoelectronic and solar cell applications of Janus monolayers and their van der Waals heterostructures, Phys. Chem. Chem. Phys. 21 (34) (2019) 18612–18621.
[37] Y.-N. Wen, M.-G. Xia, S.-L. Zhang, Bandgap engineering of Janus MoSSe monolayer implemented by se vacancy, Comput. Mater. Sci. 152 (2018) 20–27.
[38] Z. Guan, S. Ni, S. Hu, Tunable electronic and optical properties of monolayer and multilayer Janus MoSSe as a photocatalyst for solar water splitting: a first-principles study, J. Phys. Chem. C 122 (11) (2018) 6209–6216.
[39] S.-D. Guo, J. Dong, Biaxial strain tuned electronic structures and power factor in Janus transition metal dichalchogenide monolayers, Semicond. Sci. Technol. 33 (8) (2018) 085003.